IOP Conf. Series: Journal of Physics: Conf. Series **828** (2017) 012008 doi:10.1088/1742-6596/828/1/012008

Low temperature magnetic properties of frustrated pyrochlore ferromagnet $Ho_2Ir_2O_7$

Dinesh Kumar[1], S Y Chen[1], M K Lee[1], C M N Kumar[2,3], R Aldus[2] and L J Chang[1]

[1] Department of Physics, National Cheng Kung University, No. 1, University Road, Tainan 70101, Taiwan
[2] Jülich Centre for Neutron Science JCNS, Forschungszentrum Jülich GmbH, Outstation at SNS, Oak Ridge National Laboratory, Oak Ridge, Tennessee 37831, United States
[3] Laboratoire National des Champs Magnetiques Intenses CNRS, 143, avenue de Rangueil, F-31400 Toulouse, France

E-mail: dinidixit[at]gmail.com

Abstract. We have performed low temperature magnetic susceptibility, specific heat, electrical resistivity and neutron diffraction measurements to study the magnetic properties of frustrated pyrochlore ferromagnet $Ho_2Ir_2O_7$. The magnetization and dc resistivity measurement indicate metal-insulator transition near 140 K. The accumulated value of observed entropy calculated from heat capacity data is $R\ln 2$, indicating the Ho^{3+} doublet ground state. The Ir sublattice order is antiferromagnetic which is evident from the magnetization measurements. The best fit of the neutron diffraction spectra at 1.8 K shows the magnetic structures with two types of components. One of the magnetic structure is all-in-all-out type, which is due to the strong coupling between Ho^{3+} and Ir^{4+} ions and develops below 18 K. It suggests that the magnetic moment of Ho^{3+} ions align in the field of Ir^{4+}, ordering along local <111> directions. There is also a Ho^{3+} magnetic component perpendicular to <111> below 100 K. This perpendicular component may originate from the defects in the Ir sub-lattice. Defects such as Ir deficiency or an Ir atom pointing at the opposite direction will cause the emergent of the perpendicular component.

1. Introduction

The study of frustrated pyrochlore oxides having the composition $A_2B_2O_7$ is very crucial to understand the ground state that results from the competing interactions of the spins on the corners of the tetrahedron lattice. In case of the pyrochlore ferromagnet, the local Ising anisotropy makes the spins to point either into or out of the center of tetrahedron and consequently the spin configurations on ground state of one tetrahedron are six-fold degenerate having two-in-two-out structures. The pyrochlore lattice consists of a three dimensional network of corner sharing tetrahedra. If we extend this two-in-two-out structure to the entire pyrochlore lattice, we obtain a macroscopic ground state, which eventually lead to the residual entropy. The macroscopic degenerate ground state, a feature possessed by a number of frustrated materials, has been a fascinating area of research. Frustrated magnetism on site A leads to one of the remarkable phenomenon termed as “spin ice” behaviour where residual entropy has been observed in

Content from this work may be used under the terms of the Creative Commons Attribution 3.0 licence. Any further distribution of this work must maintain attribution to the author(s) and the title of the work, journal citation and DOI.
Published under licence by IOP Publishing Ltd

pyrochlore materials e.g. $Ho_2Ti_2O_7$ [1], $Dy_2Ti_2O_7$ [2], $Ho_2Sn_2O_7$ [3]. For the pyrochlore lattice, it is a well-established fact that antiferromagnetic interactions lead to the high degree of geometrical frustration [4]. Interestingly it is also been observed that even in case of ferromagnetic interaction in pyrochlore lattice, the frustration may arise due to the strong single-ion anisotropy [5].
The iridium based pyrochlore compounds, $R_2Ir_2O_7$ (R = Pr, Nd, Sm and Eu) have been investigated and a metal-nonmetal changeover has been observed in these compounds [6]. The Ir^{4+} ions containing five *5d* electrons differ from identical Mo^{4+} and Ru^{4+} ions as follows: Ir^{4+} has low spin $S = ½$ configuration, while Mo^{4+} and Ru^{4+} have $S = 1$ configuration and consequently Ir^{4+} brings about different properties. In this paper, we present the low temperature magnetic properties of frustrated pyrochlore $Ho_2Ir_2O_7$. The magnetization measurements indicate metal-insulator transition near 140 K. Neutron diffraction experiments reveal two types of the components of Ho^{3+} in the magnetic structure of pyrochlore $Ho_2Ir_2O_7$.

2. Experimental details

Polycrystalline samples of $Ho_2Ir_2O_7$ have been prepared using conventional solid-state synthesis technique. The starting materials were Ho_2O_3 (99.99%) powder and IrO_2 (99.99%) powder in the ratio 1:2 respectively. The materials were grinded well with a mortar and pestle and we pre-sintered the samples at 800^0 C for 12 hours. After pre-sintering of the samples, we pelletized the samples and heated at 1100^0 C for 20 days. The phase purity of samples is confirmed with synchrotron X-ray diffraction measurements. The dc magnetization is performed with a superconducting quantum interference device (SQUID) magnetometer (Quantum Design, USA) for various temperatures down to 2 K and magnetic fields up to 5 T. The specific heat measurement is performed using a relaxation method in a physical property measurement system (PPMS) (Quantum Design, USA) down to 1.8 K. The AC susceptibility measurements has been performed with PPMS with H_{ac} = 10 Oe superimposed on various dc magnetic fields up to 2 T, in the temperature range of 2 K - 30 K. Neutron powder diffraction measurements were carried out on the time-of-flight powder diffractometer POWGEN at the Spallation Neutron Source, Oak Ridge National Laboratory. Diffraction data were collected with the center wavelength 1.066 Å. Rietveld refinements for structures of $Ho_2Ir_2O_7$ were performed using the FullProf program.

3. DC magnetization measurements

Temperature dependence of the dc susceptibility of $Ho_2Ir_2O_7$ at 50 Oe and 1 kOe in the temperature range 50 K – 300 K is shown in figure 1. The ZFC and FC curves at 1 kOe are observed to be separated around 141 K. This ZFC-FC behaviour is consistent with the earlier reported studies on the family of these compounds, indicating that it shows metal-insulator transition (MIT) [7]. The shape of FC curve below T_{MI} depends upon the preparation of the sample. In our case, below T_{MI}, FC lies above the ZFC curve for both field values. (Note that FC and ZFC for H = 1 kOe have been divided by a factor of 1.65 for scaling purposes). One interesting feature of the FC curve at 1 kOe is that it starts separating apart ZFC curve around 225 K, 84 K higher than the T_{MI}. Previous studies have reported similar effects for metallic pyrochlore compound $Pr_2Ir_2O_7$, where resistivity starts to increase below T_{MI} [8]. This effect is attributed to the enhanced magnetic scattering of the charge carriers while approaching the magnetic ordering, due to spin-ice behaviour in a frustrated pyrochlore. The temperature dependence of inverse susceptibility (not shown here) and the Curie-Weiss law fitting of H = 50 Oe data give magnetic moment of Ho^{3+} = 8.362(1) μ_B and θ_w = 1.9 K, indicating the ferromagnetic coupling of spins in $Ho_2Ir_2O_7$.

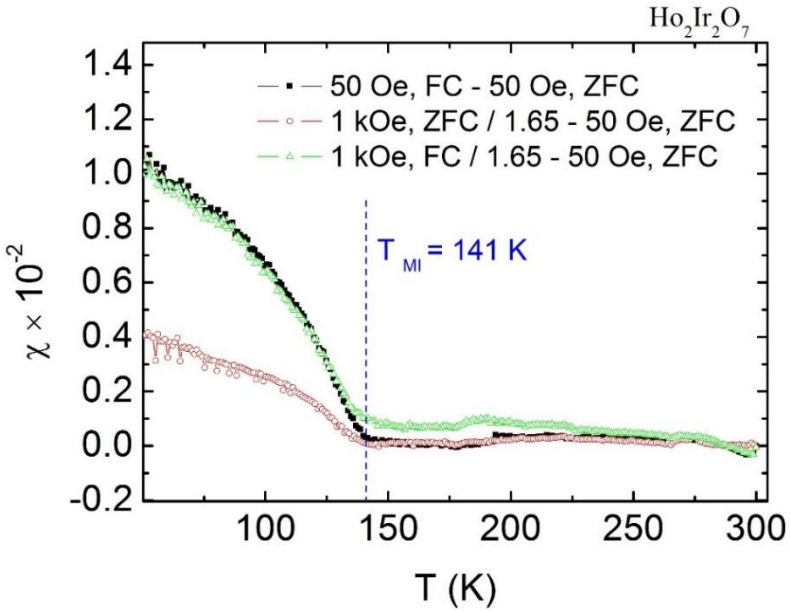

Figure 1: Temperature dependence of the susceptibility of $Ho_2Ir_2O_7$ at H = 50 Oe and 1 kOe. The data for 1 kOe is divided by a factor 1.65 for data scaling. The dotted blue line represents metal insulator transition temperature (T_{MI}) ~ 141 K. The data for 50 Oe (ZFC) is subtracted from each data set.

4. AC Susceptibility Measurements

Figures 2(a) and 2(b) show the temperature dependence of the real (χ') and imaginary (χ'') parts of the ac susceptibility of $Ho_2Ir_2O_7$ for H_{dc} = 0.7 T and H_{ac} = 10 Oe and under different ac field frequencies ranging between 10 Hz – 10 kHz. As shown in figure 2(a), χ' shows a peak near 5 K, which is consistent with the earlier published results of spin-ice materials and this peak is associated with the dynamic spin freezing at the low temperature [3,9,10]. From figure 2(b) we observed that χ'' shows a broad peak around 6 K, which is also associated with freezing of spins at the low temperature. The maxima in χ' and χ'' decreases with the increase in the ac frequency which is expected for spin freezing.

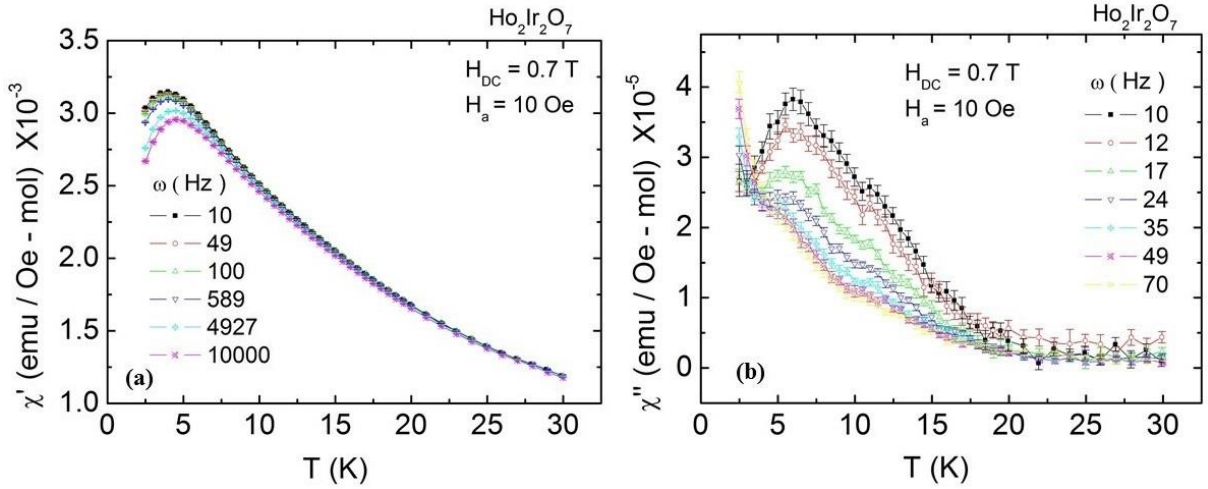

Figure 2: (a) Temperature variation of the real part of the ac susceptibility (χ') of $Ho_2Ir_2O_7$ at various measurement frequencies ranging between 10 Hz – 10 kHz with H_{dc} = 0.7 T and H_{ac} = 10 Oe. (b) Temperature variation of the imaginary part of the ac susceptibility (χ'') of $Ho_2Ir_2O_7$ at various measurement frequencies ranging between 10 Hz – 70 Hz with H_{dc} = 0.7 T and H_{ac} = 10 Oe.

The monotonic decrease in the in χ' and χ'' with increase in the temperature is in well agreement with the published results for the spin-ice materials [3]. We also observed that peak in χ'' shifts to the lower temperature with increase in the ac frequency which indicates the relaxation of the magnetization in $Ho_2Ir_2O_7$ at low temperatures.

5. Heat Capacity measurements

The magnetic contribution to the specific heat (C_m) is obtained by subtracting lattice contribution (specific heat of pyrochlore $Lu_2Sn_2O_7$), and nucleon hyperfine contribution, which has been estimated from Schottky specific heat, from the total specific heat (C_p) of $Ho_2Ir_2O_7$ in zero field. The magnetic entropy is calculated by integrating C_m/T over temperature using the formula: $\Delta S_m = \int_{T'}^{T''} \frac{C}{T}\, dT$, where T' and T'' are the initial and final temperature taken for integration interval. As we can observe from the temperature dependence of entropy (as shown in figure 3), zero-point entropy of R/2 ln3/2 does not appear in $Ho_2Ir_2O_7$ and ΔS_m is saturated near 30 K and attains the value 5.92 J/mol-K, which is slightly more than spin freezing condition Rln2 = 5.76 J/mol-K. Similar results are reported for $Dy_2Ir_2O_7$ [6]. In case of $Dy_2Ir_2O_7$ the spin freezing condition is obtained near 20 K.

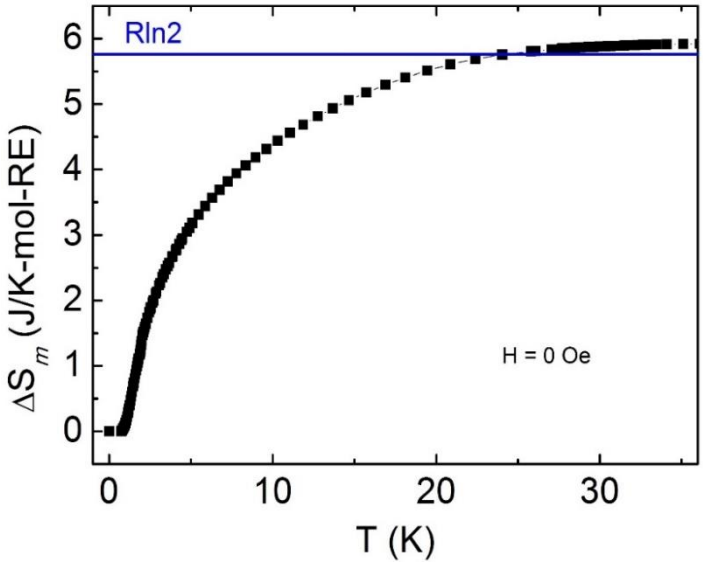

Figure 3: The temperature variation of the magnetic entropy at H = 0 Oe in the temperature range 1.8 K – 45 K.

6. Neutron diffraction measurements

Neutron powder diffraction experiments had been carried out on $Ho_2Ir_2O_7$ at various temperatures (the detailed results to be published elsewhere). Figure 4 shows the Reitveld refinement data on $Ho_2Ir_2O_7$ at T = 29 K. The red dots represent the experimental data. The solid black line is the theoretically calculated intensity. The peaks (420) and (222) might be possibly appear because of the lattice defects and not from the magnetic structure. The blue curve represents the difference of both values. The best fit of the neutron diffraction spectra at 1.8 K shows the magnetic structures with two types of components. One of the magnetic structure is all-in-all-out type, which is due to the strong coupling between Ho^{3+} and Ir^{4+} ions and develops below 18 K. It suggests the magnetic moment of Ho^{3+} ions align in the field of Ir^{4+} ordering along local <111> directions [11,12]. Another magnetic component of Ho^{3+}, perpendicular to <111> is observed below 100 K. This perpendicular component may originate from the defects in the Ir sublattice. Defects such as Ir deficiency or an Ir atom pointing at the opposite direction will cause the emergent of the perpendicular component [11].

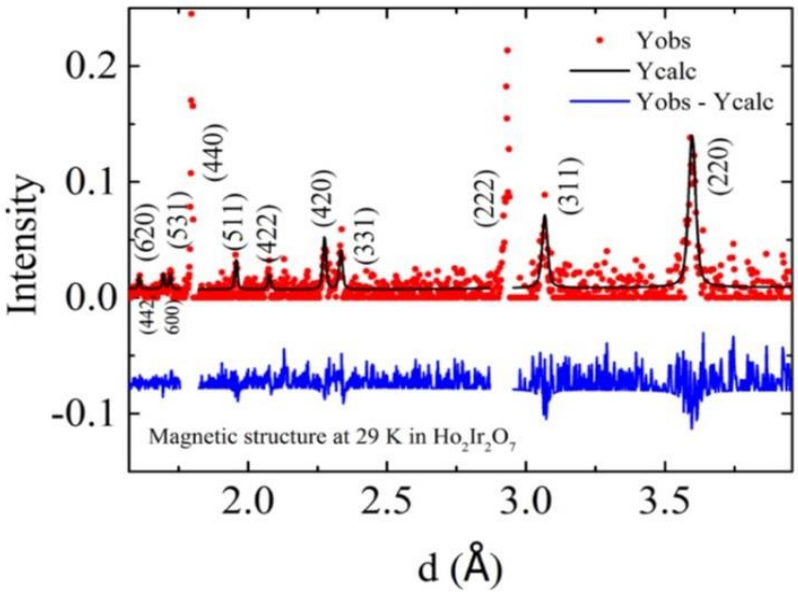

Figure 4: Reitveld refined neutron diffraction data of $Ho_2Ir_2O_7$ at T = 29 K. The red dots represent the observed intensity; black curve represent the theoretically calculated intensity and the blue curve represent the difference of both.

7. Resistivity measurements

We have performed resistivity measurements with standard four probe method. The temperature variation of the resistivity is shown in figure 5(a) in the temperature range 1.85 K – 7 K and under various magnetic field values ranging up to 5 T. The sample shows insulating behavior at low temperature (1.85 K) and H = 0 Oe. We have observed that with the increase in the field, the electrical

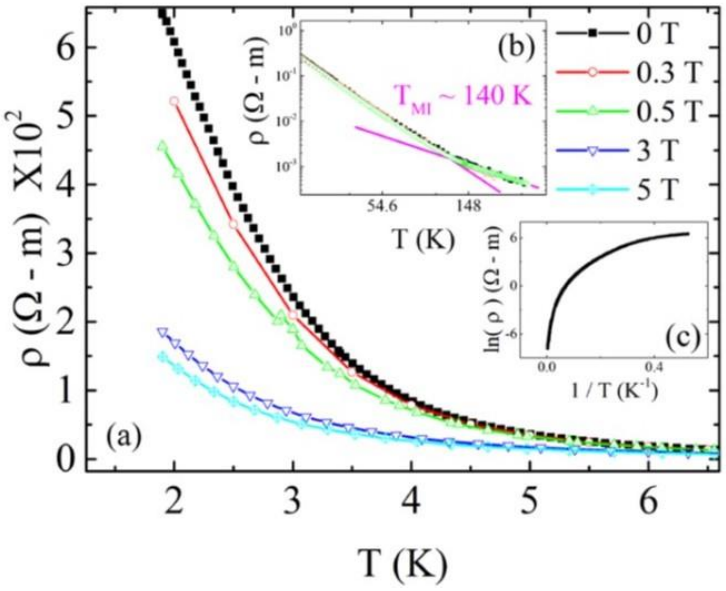

Figure 5: (a) Temperature variation of the electrical resistivity at various magnetic fields ranging up to 5 T. (b) Temperature variation of the resistivity at high temperatures indicating the metal-insulator transition near 140 K. (c) 1/T variation of the ln(ρ) to analyse thermistor behaviour of $Ho_2Ir_2O_7$.

behavior of the $Ho_2Ir_2O_7$ sample changes from insulator to the metallic behavior. Figure 5(b) shows the temperature variation of the resistivity at the high temperature and indicates the metal-insulator transition near 140 K. Further we have analyzed the thermistor behavior of $Ho_2Ir_2O_7$ as shown in the figure 5(c) and find that 1/T variation of ln(ρ) does not follow the common semiconductor thermistors formula $1/T = A + B \ln(\rho) + C [\ln(\rho)]^3$ where A, B and C are constants [13].

8. Conclusion

In conclusion, we have performed low temperature ac and dc susceptibility, specific heat, electrical resistivity and neutron diffraction measurements to study the magnetic properties of frustrated pyrochlore ferromagnet $Ho_2Ir_2O_7$. The dc magnetization and resistivity measurements show metal-insulator transition near 140 K. The total entropy accumulated from heat capacity data is Rln2, which indicates the Ho^{3+} doublet ground state. The Ir sublattice orders is the antiferromagnetic which is evidenced by the magnetization measurements. The magnetic structures with two types of components are present in the best fit of the neutron diffraction spectra at 1.8 K. One of the magnetic structure component is all-in-all-out configuration of Ising spins, along local <111> axes and develops below 18 K. There is also a component of magnetic structure, which is perpendicular to <111> axes. The perpendicular component of the magnetic structure may possibly originate from the defects in the Ir sub-lattice.

Acknowledgements

The authors would like to acknowledge financial support provided by Ministry of Science and Technology (MOST), Taiwan under project numbers 'MOST 104-2112-M-006-010-MY3' and 'MOST 104-2119-M-006-017-MY3'. The authors also gratefully acknowledge the financial support provided by JCNS to perform the neutron scattering measurements at the Spallation Neutron Source (SNS), Oak Ridge, USA. Part of the research conducted at SNS was sponsored by the Scientific User Facilities Division, Office of Basic Energy Sciences, US Department of Energy.

References

[1] Harris M J, Bramwell S T, McMorrow D F, Zeiske T and Godfrey K W 1997 *Phys. Rev. Lett.* **79** 2554
[2] Ramirez A P, Hayashi A, Cava R J, Siddharthan R and Shastry*et* B S 1999 *Nature* **399** 333
[3] Matsuhira K, Hinatsu Y, Tenya K and Sakakibara T 2000 *J. Phys.: Condens. Matter* **12** L649
[4] Harris M J and Zinkin M P 1996 *Mod. Phys. Lett. B* **10** 417
[5] Harris M J, Bramwell S T, Zeiske T, McMorrow D F, King P J C 1998 *J. Magn. Mag. Materials* **177** 757
[6] Yanagishima D and Maeno Y 2001 *J. Phys. Soc. Japan* **70** 2880
[7] Matsuhira K, Wakeshima M, Hinatsu Y and Takagi S 2011 *J. Phys. Soc. Japan* **80** 094701
[8] Nakatsuji S, Machida Y, Maeno Y, Tayama T, Sakakibara T, Duijn J van, Balicas L, Millican J N, Macaluso R T and Chan J Y 2006 *Phy. Rev. Lett.* **96** 087204
[9] Matsuhira K, Y Hinatsu Y and Sakakibara T 2001 *J. Phys.: Condens. Matter* **13** L737
[10] Lau G C, Freitas R S, Ueland B G, Muegge B D, Duncan E L, Schiffer P and Cava R J 2006 *Nature Physics* **2** 249-253
[11] Lefrançois E, Simonet V, Ballou R, Lhotel E, Hadj-Azzem A, Kodjikian S, Lejay P, Manuel P, Khalyavin D and Chapon L C 2015 *Phys. Rev. Lett*. **114** 247202
[12] Tomiyasu K, Matsuhira K, Iwasa K, Watahiki M, Takagi S, Wakeshima M, Hinatsu Y, Yokoyama M, Ohoyama K, and Yamada K 2012 *J. Phys. Soc. Japan* **81** 034709
[13] Steinhart J S and Hart S R 1968 Deep Sea Research and Oceanographic Abstracts **15** 497-503